DOI: 10.65731/ama/2026-0069

TIME-DELAY CONTROL-BASED FRACTIONAL-ORDER SLIDING MODE FOR TRAJECTORY TRACKING OF A PARALLEL DELTA ROBOT: REAL-TIME APPLICATION

Someya AMRANE*, Chems Eddine BOUDJEDIR, Djamel BOUKHETALA***

*Laboratory of Process Control Ecole Nationale Polytechnique (ENP), Algiers, Algeria
**LRPE Laboratory University of Science and Technology Houari Boumediene (USTHB) Algiers, Algeria

someya.amrane@g.enp.edu.dz, chemseddine.boudjedir@usthb.edu.dz, djamel.boukhetala@g.enp.edu.dz

received 16 November 2025, revised 14 July 2026, accepted 26 July 2026

Abstract: In this article, a time delay control-based fractional-order sliding mode (TDCFOS) approach is proposed for the trajectory tracking of a parallel Delta robot. The complex, nonlinear, and unknown dynamics of the robot are estimated using the time-delay estimation (TDE) method, which provides a model-free control structure and avoids the need for precise dynamic modeling. The use of a fractional-order sliding mode increases the flexibility of the controller and improves the tracking error when compared with conventional integer-order schemes, particularly under challenging conditions, such as increased operating speed. The stability of the closed-loop system is rigorously established through a Lyapunov-based analysis, ensuring reliable and robust performance under uncertainties and external perturbations. Experimental validations conducted on a Delta robot confirm that the proposed TDCFOS approach outperforms the traditional time-delay-based integer-order sliding mode controller (TDCIOS) in terms of tracking performance. Across two experimental scenarios involving all three robot joints, the proposed controller achieves reductions in root mean square error (RMSE) of 49% and 50.5%, and maximum absolute error (MAE) of 38% and 45.5%, respectively, compared with the TDCIOS controller.

Key words: time delay, fractional-order, sliding mode, trajectory tracking, delta robot

1. INTRODUCTION

Parallel robots have gained recognition in diverse industries, including manufacturing, aerospace and pharmaceuticals. Their unique advantages, such as high accuracy, speed, and payload capacity, contribute to enhanced productivity, making them well-suited for a wide range of applications within these sectors [1], [2]. Clavel's Delta robot, renowned for its parallel kinematic structure, plays an essential role in the industrial and surgical fields. Its ability to perform fast, precise movements makes it invaluable for many tasks. Researchers are actively investigating ways of improving its precision for complex tasks, and thus extending its field of application.

Classical PD (Proportional Derivative), PID (Proportional Integral Derivative), and PD plus feedforward controllers [3] have found wide application in robot control. However, these schemes do have some limitations due to their highly coupled dynamics, resulting in a lack of accuracy for tasks that require high precision. To effectively compensate the nonlinearity and highly coupled dynamics, several advanced model-based controllers have been proposed, such as sliding mode controllers (SMC) [4–6], adaptive controller [7], and iterative controller [8].

Recently, finite-time and fixed-time control methods have attracted significant attention [9–11]. While finite-time control guarantees convergence within a settling time that depends on the initial tracking error, fixed-time control ensures convergence within a settling time independent of the initial conditions. Nevertheless, most existing methods are model-based, and their performance may degrade in the presence of modeling uncertainties. To overcome the previously mentioned problem, model-free controllers offer an alternative solution that does not depend on the mathematical model of the system. Indeed, numerous scientific works have been conducted in this field, such as reinforcement learning [12], neural network control [13] and fuzzy logic control [14]. In [15] and [16], fuzzy logic is integrated with metaheuristic optimization algorithms, such as the Flower Pollination Algorithm (FPA) and Harmonic Search (HS), to optimize controller parameters and enhance control performance. However, these approaches require intensive optimization procedures, which increase computational cost.

One of the most interesting model-free controllers is time delay control (TDC), which relies significantly on time delay estimation (TDE) to approximate the unknown dynamic model using only the output signal. TDC has been successful in several applications, such as exoskeleton robots [17], underwater vehicles [18], and robot manipulators [19]. Nevertheless, tracking accuracy is not satisfactory due to the existence of the time delay estimation error. To compensate for time-delay estimation (TDE) errors, sliding mode control has been combined with time-delay control (TDC) in various studies [20], [21]. In [22], a finite-time sliding mode control scheme integrated with TDC was proposed to improve tracking performance under uncertainties. To further enhance convergence and address singularity issues, nonsingular terminal sliding mode control was introduced in [23]. More recently, fixed-time control strategies have been introduced, as in [24], which guarantee convergence within a bounded time independent of initial conditions.

The above-mentioned approaches have focused on integer-order schemes, which have demonstrated high control performance. However, fractional-order controllers have gained significant interest due to their ability to offer better accuracy. By incorporating fractional-order elements, additional adjustable parameters are introduced, leading to enhanced flexibility [25–27]. This results in higher tracking accuracy and improved control performance. Recent implementations of Fractional-Order Sliding Mode Control (FOSMC) have provided evidence of its success in practical control applications [28–32]. In [33], mathematical analysis indicates that fractional-order reduces reaching time.

These studies demonstrate the improved performance achieved by the fractional-order sliding mode controller and highlight its effectiveness in real-world control scenarios.

The proposed TDCFOS control law guarantees robustness and effectively addresses TDE errors, thereby improving tracking performance. Fractional-order control increases the degrees of freedom of the controller, making it more flexible. Moreover, fractional-order control offers the advantage of reducing large errors faster than integer-order control. The main contributions of this article can be summarized as follows:

– The synthesis of a time-delay controller-based fractional-order sliding mode to enhance the tracking performance of robot manipulators.
– The asymptotic stability of the sliding surface has been proven using Lyapunov analysis.
– The experimental results validate the improved trajectory tracking accuracy of the proposed approach compared to the TDCIOS method.

The remaining sections of this article are organized as follows: Section II presents the problem statement. In Section III, the proposed time delay control-based fractional-order sliding mode is introduced, along with stability analysis. Section IV presents the experimental results. Finally, Section V concludes this paper.

2. PROBLEM STATEMENT

The aim of this study is to design a TDCFOS control law that ensures that the Delta robot's joint vector, denoted by q_t, closely follows the desired joint vector $q_{d,t}$ over time.

The dynamic model of a robot manipulator with n-degree of freedom (n-DOF) is described as follows:

$$M(q_t)\ddot{q_t} + C(q_t, \dot{q}_t)\dot{q}_t + G(q_t) + d_t = \tau_t \tag{1}$$

$q_t \in R^n$ represents the generalized joint vector, The inertia matrix is denoted as $M(q_t) \in R^{n\times n}$, The matrix resulting from centrifugal and Coriolis forces is repre- sented by $C(q_t, \dot{q}_t) \in R^{n\times n}$. The term $G(q_t) \in R^n$ refers to the gravitational vector, $d_t \in R^n$ is the external disturbances and $\tau_t \in R^n$ denotes the joint torque.

The expression (1) can be restated as follows:

$$(M(q_t) - \bar{M})\ddot{q_t} + \bar{M}\ddot{q_t} + C(q_t, \dot{q}_t)\dot{q}_t + G(q_t) + d_t = \tau_t \tag{2}$$

where $\bar{M}(q_t) \in R^{n\times n}$ is a positive diagonal matrix consistent with the robot's dynamics.

The expression (2) can be reformulated as follows:

$$\ddot{q_t} = N_t + \bar{M}^{-1}\tau_t \tag{3}$$

with

$$N_t = \bar{M}^{-1}[C(q_t, \dot{q}_t)\dot{q}_t + G(q_t) + d_t + (M(q_t) - \bar{M})\ddot{q_t}] \tag{4}$$

Since the value of N_t depends on system dynamics and unknown external disturbances, estimating N_t is a complex task.

Therefore, the TDE technique is used to calculate its approximate value $\widehat{N}_t$ as follows

$$\widehat{N}_t = N_{t-L} = \ddot{q}_{t-L} - \bar{M}^{-1}\tau_{t-L} \tag{5}$$

where L represents the chosen delay time, which is typically set equal to the sampling time and $\ddot{q}_{t-L}$ is the past acceleration. e_t and $\dot{e}_t$ are the tracking position and velocity error defined as

$$e_t = q_{d,t} - q_t \tag{6}$$

$$\dot{e}_t = \dot{q}_{d,t} - \dot{q}_t \tag{7}$$

where $q_t \in R^n$ is the desired joint trajectory vector. The conventional TDC technique is given as follows

$$\tau_t = \bar{M}\left(\ddot{q}_{t-L} + k_d\dot{e}_t + k_p q_t\right) + \tau_{t-L} - \bar{M}\ddot{q}_{t-L} \tag{8}$$

Since the TDC controller operates on the basis of delayed information, it causes a delay estimation error (TDE), characterized as follows

$$\widehat{N}_t - N_t = H_t = -\bar{M}^{-1}\left(\ddot{e}_t + k_d\dot{e}_t + k_p\dot{e}_t\right) \tag{9}$$

To demonstrate the boundedness of the TDE error, (8) is substituted into (3) as follows:

$$\ddot{q_t} = N_t + \bar{M}^{-1}\bar{M}\left(\ddot{q}_{t-L} + k_d\dot{e}_t + k_p q_t - \ddot{q}_{t-L}\right) + \bar{M}^{-1}\tau_{t-L} \tag{10}$$

Therefore,

$$\ddot{q}_t = N_t + \bar{M}^{-1}\bar{M}\varphi + \bar{M}^{-1}\tau_{t-L} \tag{11}$$

where

$$\varphi = \ddot{q}_{t-L} + k_d\dot{e}_t + k_p q_t - \bar{M}\ddot{q}_{t-L} \tag{12}$$

Using (5), (11) becomes

$$\ddot{q_t} = N_t + \bar{M}^{-1}\bar{M}\varphi + \ddot{q}_{t-L} - N_{t-L} \tag{13}$$

Thus,

$$\ddot{q_t} = H_t + \bar{M}^{-1}\bar{M}\varphi + \ddot{q}_{t-L} \tag{14}$$

Hence,

$$H_t = \ddot{q_t} - \bar{M}^{-1}\bar{M}\varphi - \ddot{q}_{t-L} \tag{15}$$

Therefore,

$$H_t = \ddot{q_t} - [\mathrm{I} - \bar{M}^{-1}\bar{M}]\ddot{q}_{t-L} - \bar{M}^{-1}\bar{M}u_t \tag{16}$$

Where,

$$u_t = \ddot{q}_{t-L} + k_d\dot{e}_t + k_p q_t \tag{17}$$

Following the derivation procedure in [31], (17) can be rewritten as follows

$$H_t = [\mathrm{I} - \bar{M}^{-1}\bar{M}]\ \mathrm{H}_{t-L} + \Delta \tag{18}$$

where Δ denotes a bounded external forcing term. From (18), if

$$||I - M^{-1}(q_t)\bar{M}|| < 1,$$

then H_t is guaranteed to be bounded according to the BIBO stability criterion [34].

Then, the TDE error is bounded as follows

$$||H_t|| < H^* \tag{19}$$

where H^* is a constant.

DOI: 10.65731/ama/2026-0069

3. CONTROL DESIGN AND CONVERGENCE ANALYSIS

3.1. Fractional calculus

Definition 1. [35]. The Riemann-Liouville definition of the fractional-order derivative is given as

$$_{RL}D^{p}_{t_{0,r}}f(t) = \left(\frac{d}{dt}\right)^{m} D^{-(m-p)}_{t_{0,t}} f(t)$$

$$= \frac{1}{\Gamma(m-p)}\left(\frac{d}{dt}\right)^{m}\int_{t_0}^{t}(t-\tau)^{m-p-1}f(\tau)d\tau, \quad t > t_0$$

Where p is the fractional-order, and m is the first integer larger than p, i.e. $m-1 \le p < m$. The Euler gamma function Γ is defined as

$$\Gamma(z) = \int_0^{\infty}\frac{t^{z-1}}{e^t}dt \tag{20}$$

The Riemann-Liouville integration is given as

$$_{RL}D^{-p}_{t_{0,r}}f(t) = \frac{1}{\Gamma(p)}\int_{t_0}^{t}(t-\tau)^{p-1}f(\tau)d\tau, \ t > t_0 \tag{21}$$

Property 1. [35]. When considering the composition of fractional derivatives given $_{a}D^{q}_{t}\left(_{a}D^{p}_{t}f(t)\right)$, the fractional derivatives commute as follows

$$_{a}D^{q}_{t}\left(_{a}D^{p}_{t}f(t)\right) = {_{a}D^{p}_{t}}\left(_{a}D^{q}_{t}f(t)\right) = {_{a}D^{p+q}_{t}}(f(t)) \tag{22}$$

If,

$q < 0, 0 \le m < p < m+1,$

and $f^{k}(a) = 0 \ for \ k = 0,1,\ldots,(r-1)$ with $r = max(n,m)$.

Definition 2. The Grunwald-Letnikov definition given below was employed during experimental analysis

$$_{a}D^{\mu}_{t}(f(t)) = \frac{_{a}d^{\mu}_{t}f(t)}{dt^{\mu}} = \lim_{h\to 0}\frac{1}{h^{\mu}}\sum_{k=0}^{N}(-1)^{k}\binom{n}{k}f(t-kh) \tag{23}$$

The Grunwald-letnikov numerical approximation provided below is used to easily handle fractional calculus when software implementation takes place

$$_{\mathrm{k-L/h}}D^{\mu}_{t}(f(\mathrm{t_k})) =\approx \frac{1}{h^{\mu}}\sum_{\mathrm{j=0}}^{\mathrm{k}}(-1)^{\mathrm{j}}\binom{\mu}{\mathrm{j}}f(\mathrm{t_{k-j}}) = \frac{1}{h^{\mu}}\sum_{\mathrm{j=0}}^{\mathrm{k}}\mathrm{c}^{\mu}_{\mathrm{j}}f(\mathrm{t_{k-j}}) \tag{24}$$

where L represents the length memory, k is the current index and h denotes the sampling period. The binomial coefficients can be calculated using the following expression

$$\mathrm{c}^{\mu}_{\mathrm{j}} = \left(1-\frac{1+\mu}{j}\right)\mathrm{c}^{\mu}_{\mathrm{j-1}} \tag{25}$$

and $\mathrm{c}^{\mu}_{0} = 1$

3.2. Control design

The fractional order surface is given as follows

$$s_t = k_d e_t + D^{1-\lambda}e_t \tag{26}$$

where k_d is a constant diagonal matrix and $0 < \lambda < 1$.

The proposed controller is given as follow

$$\tau = \tau_{\mathrm{t-L}} - \bar{M}\ddot{q}_{\mathrm{t-L}} + \bar{M}u \tag{27}$$

$$u = \ddot{q}_{d,t} + D^{1+\lambda}k_d e_t + k_{\mathrm{p}}\mathrm{sign}(s_t) \tag{28}$$

while k_d and k_{p} are diagonal positive constant matrices.

Remark 1: It can be observed from the equations (27), and (28) that the controller does not require any prior knowledge of the system's dynamics. It simply relies on delayed information thanks to the time delay controller. As a result, implementing the control scheme is straightforward.

3.3 Comparison between the proposed tdcfos and the TDCIOS

The existing TDCIOS control scheme is compared with the proposed TDCFOS. Its control law is written as follows

$$\tau = \tau_{\mathrm{t-L}} - \bar{M}\ddot{q}_{t-L} + \bar{M}(\ddot{q}_{\mathrm{d,t}} + k_d e_t + k_{\mathrm{p}}\mathrm{sign}(s_t)) \tag{29}$$

where $s_t = \dot{e}_t + k_d e_t$

Remark 2: Fractional Order Sliding Mode (FOSM) control enhances flexibility by introducing an additional degree of freedom via the differential/integrator operator. This allows the introduction of additional tuning parameters, resulting in increased accuracy and robustness. Research in [32] illustrates, through mathematical analysis that fractional-order control leads to shorter reaching times compared to traditional integer-order methods, as well as smaller tracking error.

Remark 3: The influence of fractional-order is particularly pronounced due to the avoidance of the singularity problem, a benefit that arises from the fractional-order λ being between 0 and 1.

3.4 Convergence analysis

Theorem: Consider the robot manipulator with n-DOF (1), under the designed TDCFOS (29), then the sliding surface converges asymptotically to zero, i.e., $\lim_{t\to\infty} s_t = 0$

Proof

The Lyapunov function candidate is defined as

$$v = \frac{1}{2}s_t^T s_t \tag{30}$$

By derivating the Lyapunov function with respect to time, we obtain

$$\dot{v} = s_t^T \dot{s}_t \tag{31}$$

Thus

$$\dot{v} = s_t^T(k_d\dot{e}_t + D^{1-\lambda}\dot{e}_t) \tag{32}$$

$$\dot{v} = s_t^T(k_d\dot{e}_t + D^{-\lambda}(\ddot{\mathrm{q}}_{\mathrm{d,t}} - \ddot{q}_t)) \tag{33}$$

By substituting (3) into (33), we get

$$\dot{v} = s_t^T(k_d\dot{e}_t + D^{-\lambda}(\ddot{\mathrm{q}}_{\mathrm{d,t}} - (N_t + \bar{\mathrm{M}}^{-1}\tau_t))) \tag{34}$$

By using (27) and (28), we obtain

$$\dot{v} = s_t^T(k_d\dot{e}_t + D^{-\lambda}(\ddot{q}_{\mathrm{d},t} - (N_t + \bar{M}^{-1}(\tau_{t-\mathrm{L}} - \bar{M}\ddot{q}_{\mathrm{t-L}} + \bar{\mathrm{M}}(\ddot{q}_{\mathrm{d},t} + D^{1+\lambda}k_d\mathrm{e_t} + k_{\mathrm{p}}\mathrm{sign}(s_t)))) \tag{35}$$

Hence

$$\dot{v} = s_t^T(k_d\dot{e}_t + D^{-\lambda}\ddot{q}_{\mathrm{d},t} - D^{-\lambda}N_t + D^{-\lambda}\bar{M}^{-1}\tau_{t-\mathrm{L}} + D^{-\lambda}\ddot{q}_{\mathrm{t-L}} - D^{-\lambda}\ddot{q}_{\mathrm{d},t} - D^{-\lambda}D^{1+\lambda}k_d\mathrm{e_t} - D^{-\lambda}k_{\mathrm{p}}\mathrm{sign}(s_t))) \tag{36}$$

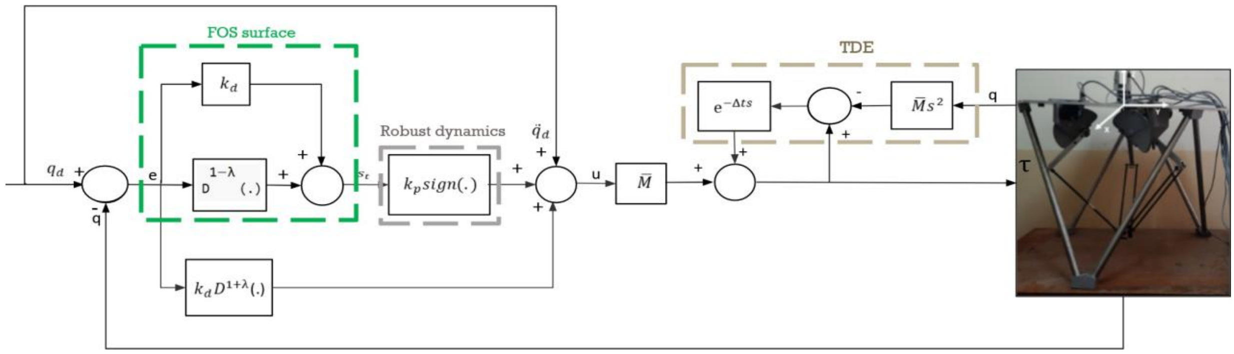

Fig. 1. Bloc diagram of the proposed TDCFOS controller

In the conducted experiments, the actual trajectory starts from the same point as the desired trajectory, this result in: $e^{k}(0) = 0, k = 0, 1.$

Therefore, from property 1, we conclude that

$$D^{-\lambda}D^{1+\lambda}e_t = D^1 e_t = \dot{e}_t \tag{37}$$

Thus

$$\dot{v} = s_t^T(k_d\dot{e}_t + D^{-\lambda}\ddot{q}_{d,t} - D^{-\lambda}N_t - D^{-\lambda}(\bar{M}^{-1}\tau_{t-L} - \ddot{q}_{t-L}) - D^{-\lambda}\ddot{q}_{d,t} - k_d\dot{e}_t - D^{-\lambda}k_p\mathrm{sign}(s_t))) \tag{38}$$

Using (5), we get

$$\dot{v} = s_t^T(D^{-\lambda}(-N_t + \hat{N}_t) - D^{-\lambda}k_p\mathrm{sign}(s_t)) \tag{39}$$

By substituting (9) in (39), we obtain

$$\dot{v} = s_t^T(D^{-\lambda}(H_t - k_p\mathrm{sign}(s_t))) \tag{40}$$

$$\dot{v} = \sum_{i=1}^{n} s_{t,i}\,(D^{-\lambda}(H_i - k_{p_i}\mathrm{sign}(s_{t,i}))) \tag{41}$$

$$\dot{v} = \sum_{i=1}^{n}(-s_{t,i}\mathrm{sign}(s_{t,i}))\,(D^{-\lambda}(k_{p_i} - H_i\mathrm{sign}(s_{t,i})) \tag{42}$$

The gain k_{p_i} can be selected as follow

$$k_{p_i} > |H_i\mathrm{sign}(s_{t,i})| \geq H^*, i = 1{:}n$$

Since the fractional integration order λ is between 0 and 1, we can conclude from definition 1 of fractional integration in (23) the following equation

$$D^{-\lambda}(k_{p_i} - H_i\mathrm{sign}(s_{t,i})) \geq \varepsilon \tag{43}$$

where ε is a positive constant parameter

Finally, by using (43), (42) becomes

$$\dot{v} \leq \sum_{i=1}^{n} -|s_{t,i}|\varepsilon \leq 0 \tag{44}$$

Therefore, $\dot{v}$ is definite negative. We can conclude that s_t converges to zero asymptotically [36].

Since

$$\sum_{i=1}^{n}|s_i| \geq \|s\|_2 = \sqrt{s^Ts} = \sqrt{2V} \tag{45}$$

Using (45), (44) becomes

$$\dot{V} \leq -\varepsilon\sqrt{2V} = -\sqrt{2}\varepsilon V^{\frac{1}{2}} \tag{46}$$

Since $0 < \frac{1}{2} < 1$, the above inequality satisfies the standard finite-time stability condition $\dot{V} \leq -cV^{\alpha}$, where $c = \sqrt{2}\varepsilon > 0$ and α= $\frac{1}{2}$. Therefore, according to the finite-time stability theorem, the sliding variable $s(t)$ converges to the origin in finite time [9].

Once the sliding variable reaches the sliding manifold, i.e., $s(t) = 0$, the tracking error dynamics reduce to

$$D^{\alpha}e(t) = -k_d e(t) \tag{47}$$

The solution of (47) can be expressed in terms of the Mittag-Leffler function as follows [37], [38]

$$e(t) = e(0)E_{\alpha}(-k_d t^{\alpha}) \tag{48}$$

where $E_{\alpha}(z) = \sum_{k=0}^{\infty}\frac{z^k}{\Gamma(\alpha k+1)}$. It is well known that for, $k_d > 0$ and $0 < \alpha < 1$,

$$\lim_{t\to\infty} E_{\alpha}(-k_d t^{\alpha}) = 0 \tag{49}$$

Therefore,

$$\lim_{t\to\infty} e(t) = e(0)\lim_{t\to\infty} E_{\alpha}(-k_d t^{\alpha}) = 0 \tag{50}$$

which proves that the tracking error converges asymptotically to the origin.

4. EXPERIMENTAL RESULT

The Delta robot is designed to achieve high precision in fast pick-and-place operations [3]. It is equipped with three brushed DC motors, featuring a 12:1 reduction ratio. Robot control algorithms were implemented using the C language, and data acquisition was carried out at a sampling frequency of 1 kHz. Table 1 shows the main dynamic and geometric parameters of the Delta robot. To evaluate the tracking accuracy of the controllers, the root-mean-square error (RMSE) and maximum absolute error (MAE) of the joints are selected as performance indices [39]. A comparative study has been conducted on the experimental results obtained for the proposed TDCFOS scheme and the TDCIOS scheme.

Tab. 1. Geometric and dynamic parameters

Parameter	Description	Value
L_a	Upper arm length	0.380 m
L_b	Forearm length	0.205 m
m_n	Travelling plate mass	0.042 Kg
m_{br}	Upper arm mass	0.098 Kg
m_{ab}	Forearms masses	0.028 Kg
m_c	Elbow mass	0.015 Kg

Table 2 presents the gain values of the proposed controller and the TDCIOS approach. To achieve a balanced compromise between tracking performance and system vibration, the chosen gains were determined by increasing one gain at a time while keeping the others fixed, and observing the system's response to identify the point at which vibration occurs. This step was performed while simultaneously monitoring the tracking performance. The experiments were carried out in two scenarios.

Tab. 2. Control parameters

Controller	Parameters	Value
TDCFOS Scheme	kd, kp, $\bar{M}$, λ	diag{1800.474, 1800.474, 1800.474} diag{5.461, 5.461, 5.461} diag{0.001, 0.001, 0.001} diag{0.1, 0.1, 0.1}
TDCIOS Scheme	kd, kp, $\bar{M}$	diag{1800.474, 1800.474, 1800.474} diag{5.461, 5.461, 5.461} diag{0.001, 0.001, 0.001}

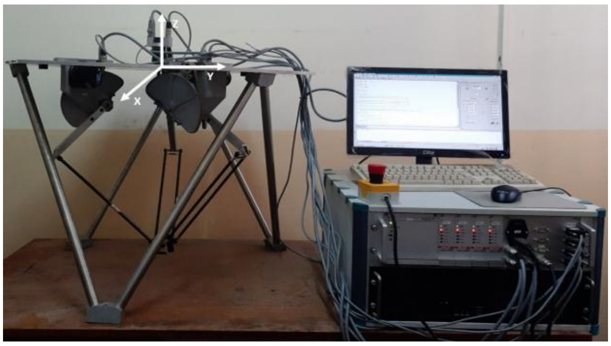

Fig. 2. Delta robot

4.1. Scenario 1

In this scenario, the maximum acceleration is set to 10 m/s2. Fig. 3 illustrates the tracking trajectory of the proposed TDC-based fractional-order sliding mode in the operational space. This trajectory adopts the shape of a semi-ellipsoid with a height of transit equal to 0.038m, passing from point (a): (0.03,0.05,0) m to point (b): (0.03, - 0.15,0) m, then back to (a), and finally from (a) to (c): (0.1,0.1, -0.41) m before returning to (a). Fig. 4 depicts the tracking error of the three joints using both the TDCIOS controller and the proposed TDCFOS. It is observed that the proposed approach achieves small tracking errors with higher accuracy compared to the other approach. The control input for the fractional-order and integer order TDC controllers shown in Fig 5 are approximately similar while staying in the admissible bounds.

Tab. 3. Tracking performance of scenario 1

Controller	Joint	TDCFOS	TDCIOS
RMSE	Joint 1	0.0143	0.0295
	Joint 2	0.0158	0.0271
	Joint 3	0.01	0.0241
MAE	Joint 1	0.058	0.012
	Joint 2	0.097	0.12
	Joint 3	0.07	0.158

Table 3 presents the RMSE and MAE of the controllers. The TDC-based FOS shows an RMS error of 0.024 and MAE equal to 0.097 which is less than 49% and 38% of those provided by the TDC based IOS method.

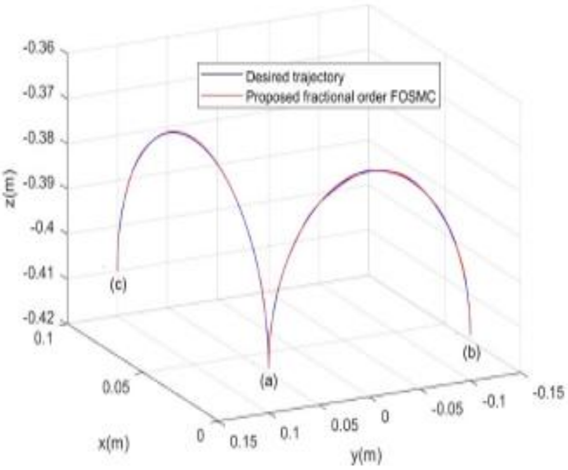

Fig. 3. Trajectory tracking in the operational space

4.1. Scenario 1

To examine the effectiveness of the TDC-based fractional-order controller under higher acceleration. An experiment was conducted with a maximum acceleration of 15 m/s2. The experimental results are illustrated in Fig. 6 and Fig. 7 where the proposed controller continues to demonstrate better tracking performance compared to the TDCIOS approach. Indeed, this superiority can be confirmed by the RMSE and MAE values presented in Table 4.

Tab. 4. Tracking performance of scenario 2

Controller	Joint	TDCFOS	TDCIOS
RMSE	Joint 1	0.011	0.017
	Joint 2	0.01	0.032
	Joint 3	0.007	0.015
MAE	Joint 1	0.117	0.1643
	Joint 2	0.079	0.2063
	Joint 3	0.137	0.2523

5. LIMITATION OF STUDY

Although the proposed controller exhibits high tracking accuracy, the complete elimination of chattering while maintaining fast convergence remains a challenging issue in sliding mode control. Therefore, the controller parameters were selected to achieve a balanced trade-off among tracking accuracy, robustness, and chattering attenuation.

6. CONCLUSIONS

This paper presents a model-free TDCFOS approach to control a Delta robot manipulator. The stability of the controller when applied to n-DOF robot manipulators is proven using the Lyapunov technique. Experiments were carried out on a Delta robot under two different accelerations to evaluate the effectiveness of the proposed scheme. A comparative study was performed with a TDC-based conventional sliding surface. The results show that the TDCFOS scheme achieves better tracking accuracy even in scenarios involving high acceleration. The proposed controller is distinguished by its ease of implementation, since it relies on the output signal.

This feature makes it a practical and suitable approach for a variety of applications. Future research will focus on proposing adaptive law and a fractional-order sliding surface to further reduce chattering and improve tracking performance.

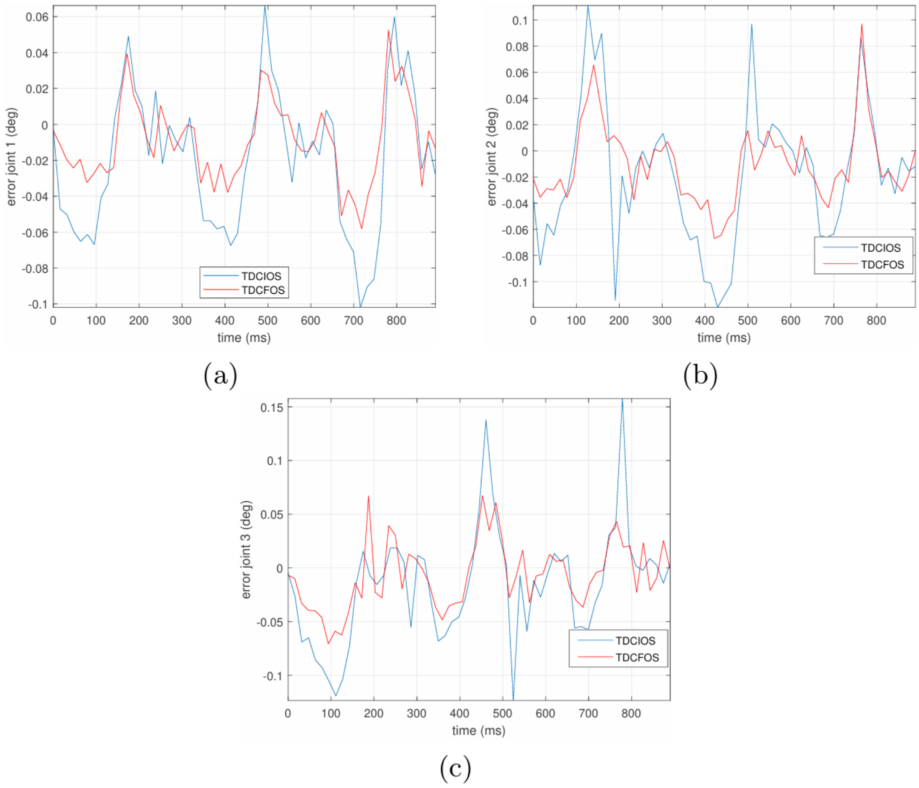

Fig. 4. Experimental tracking error for scenario 1: (a) joint 1, (b) joint 2, (c) joint 3

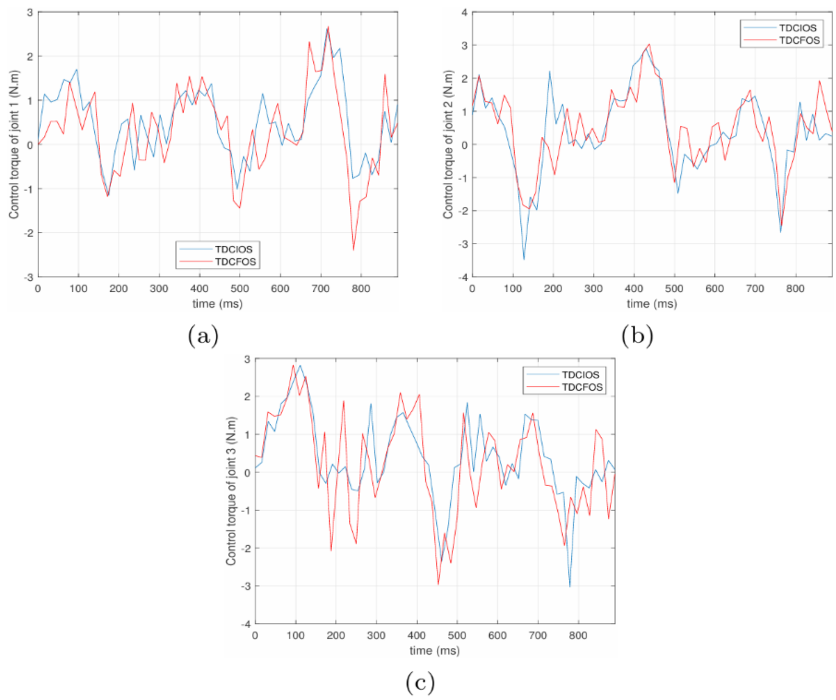

Fig. 5. Experimental control torque for scenario 1: (a) joint 1, (b) joint 2, (c) joint 3

DOI: 10.65731/ama/2026-0069

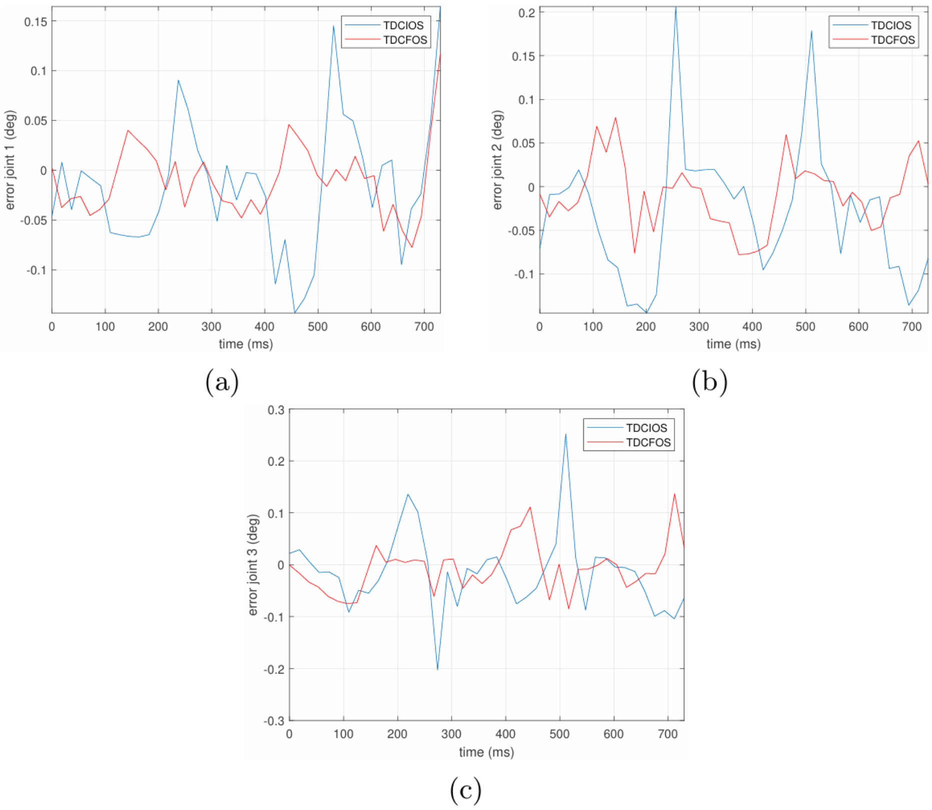

Fig. 6. Experimental tracking error for scenario 2: (a) joint 1, (b) joint 2, (c) joint

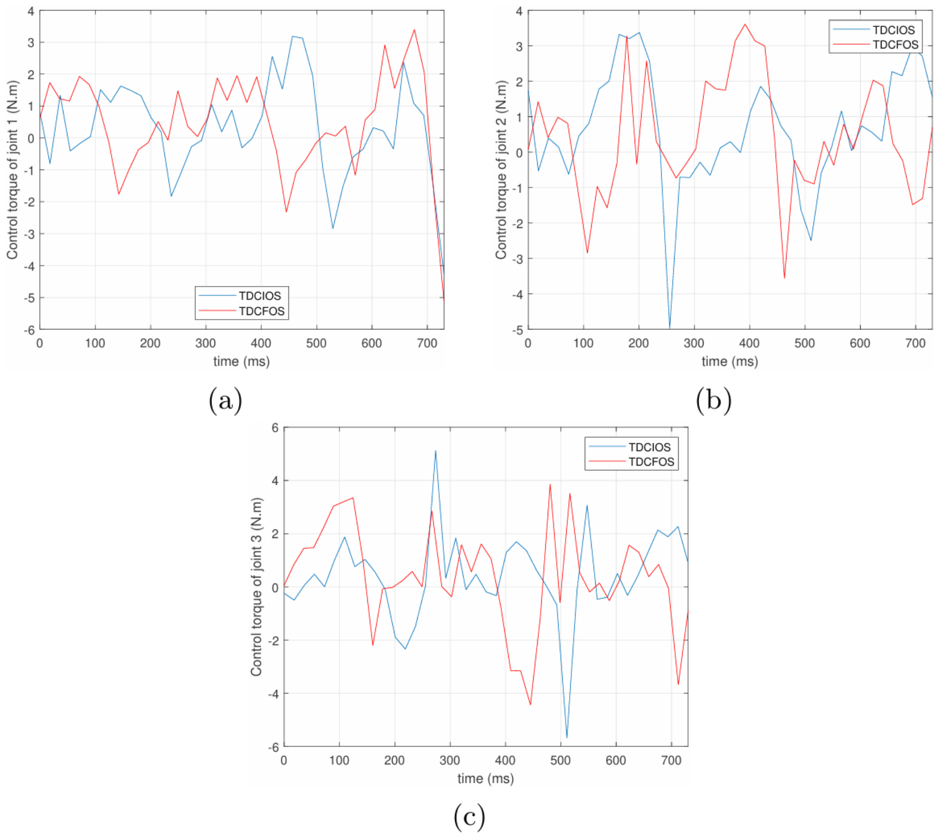

Fig. 7. Experimental control torque for scenario 2: (a) joint 1, (b) joint 2, (c) joint 3

REFERENCES

1. Clavel R. Conception d'un robot parallèle rapide à 4 degrés de liberté [technical report]. Lausanne: EPFL; 1991.
2. Brinker J, Corves B. A survey on parallel robots with delta-like architture. In: Proceedings of the 14th IFToMM World Congress; 2015: 407-14.
3. Codourey A. Dynamic modelling and mass matrix evaluation of the delta parallel robot for axes decoupling control. In: Proceedings of IEEE/RSJ International Conference on Intelligent Robots and Systems (IROS'96). 1996;3: 1211-8.
4. Boudjedir CE, Boukhetala D, Bouri M. Nonlinear PD plus sliding mode control with application to a parallel delta robot. J Electr Eng. 2018;69(5):329-36.
5. Alhaddad M. Adaptive motion control of a mobile wheeled robot taking into account the nonideality of the drives. J Comput Syst Sci Int. 2022;61:868-83.
6. Boudjedir CE, Boukhetala D, Bouri M. Iterative learning control of multivariable uncertain nonlinear systems with nonrepetitive trajectory. Nonlinear Dyn. 2019;95(3):2197-208.
7. Reshetnikov AG, Ulyanov V, Ulyanov S. Intelligent robust control of autonomous robot: quantum self-organization of imperfect knowledge bases experiment. J Comput Syst Sci Int. 2023;62:884-902.
8. Kormushev P, Calinon S, Caldwell DG. Reinforcement learning in robotics: applications and real-world challenges. Robotics. 2013;2(3):122-48.
9. Song Y, Ye H, Lewis FL. Prescribed-time control and its latest developments. IEEE Trans Syst Man Cybern Syst. 2023;53(7):4102-16.
10. Zhang L, Su Y, Wang Z, Wang H. Fixed-time terminal sliding mode control for uncertain robot manipulators. ISA Trans; 2024.
11. Boudjedir CE. A widely-practical model-free prescribed time control for trajectory tracking of n-DOF robot manipulators. Eur J Control. 2025;86.
12. Patel HR, Shah VA. A metaheuristic approach for interval type-2 fuzzy fractional order fault-tolerant controller for a class of uncertain nonlinear system. Automatika. 2022;63(4):656-75.
13. Patel HR, Shah VA. Application of metaheuristic algorithms in interval type-2 fractional order fuzzy TID controller for nonlinear level control process under actuator and system component faults. Int J Intell Comput Cybern. 2021;14(1):33-53.
14. Zha W, Zhang H, Xu X. Manipulator trajectory tracking with a neural network adaptive control method. Math Probl Eng. 2021;2021:1-8.
15. Brahmi B, Saad M, Ochoa-Luna C, Rahman MH, Brahmi A. Adaptive tracking control of an exoskeleton robot with uncertain dynamics based on estimated time-delay control. IEEE/ASME Trans Mechatron. 2018;23(2):575-85.
16. Cho GR, Li JH, Park D, Jung JH. Robust trajectory tracking of autonomous underwater vehicles using back-stepping control and time delay estimation. Ocean Eng. 2020;201:107131.
17. Van M, Ge SS, Ren H. Finite time fault tolerant control for robot manipulators using time delay estimation and continuous nonsingular fast terminal sliding mode control. IEEE Trans Cybern. 2016;47(7): 1681-93.
18. Boudjedir CE, Bouri M, Boukhetala D. An enhanced adaptive time delay control-based integral sliding mode for trajectory tracking of robot manipulators. IEEE Trans Control Syst Technol. 2023;31(3):1042-50.
19. Zhang Z, Li X, Wang X, Zhou X, An J, Li Y. TDE-based adaptive integral sliding mode control of space manipulator for space-debris active removal. Aerospace. 2022;9(2):105.
20. Song T, Fang L, Wang H. Model-free finite-time terminal sliding mode control with a novel adaptive sliding mode observer of uncertain robot systems. Asian J Control. 2022;24(3):1437-51.
21. Liang X, Wan Y, Zhang C, et al. Task space trajectory tracking control of robot manipulators with uncertain kinematics and dynamics. Math Probl Eng;2017.
22. Kang E, He J, Wang Y. Design of non-singular fast terminal sliding mode controller for permanent magnet synchronous motors. Electr Mach Control. 2021;25:58-64.
23. Sun J, Wang J, Yang P, Guo S. Fractional-order prescribed performance sliding mode control with time delay estimation for wearable exoskeletons. IEEE Trans Ind Inform; 2022.
24. Song S, Liu Z, Yuan S. Nonsingular sliding mode control of PMSM-drive servo systems: a novel fast fixed-time scheme. IEEE Trans Power Electron. 2026;41(4):4588-93.
25. Aouiti C, Cao J, Jallouli H, Huang C. Finite-time stabilization for fractional-order inertial neural networks with time varying delays. Nonlinear Anal Model Control. 2022;27(1):1-18.
26. Dumlu A. Design of a fractional-order adaptive integral sliding mode controller for the trajectory tracking control of robot manipulators. Proc Inst Mech Eng Part I J Syst Control Eng. 2018;232(9):1212-29.
27. Jie W, Yudong Z, Yulong B, Kim HH, Lee MC. Trajectory tracking control using fractional-order terminal sliding mode control with sliding perturbation observer for a 7-DOF robot manipulator. IEEE/ASME Trans Mechatron. 2020;25(4):1886-93.
28. Eray O, Tokat S. The design of a fractional-order sliding mode controller with a time-varying sliding surface. Trans Inst Meas Control. 2020;42(16):3196-215.
29. Sachan S, Swarnkar P. Intelligent fractional order sliding mode based control for surgical robot manipulator. Electronics. 2023;12(3):729.
30. Rasouli M, Zare A, Yaghoubi H, Alizadehsani R. Designing a secure mechanism for image transferring system based on uncertain fractional order chaotic systems and NLFPID sliding mode controller. Axioms. 2023;12.
31. Baek J, Cho S, Han S. Practical time-delay control with adaptive gains for trajectory tracking of robot manipulators. IEEE Trans Ind Electron. 2018;65(7):5682-92.
32. Yin C, Chen YQ, et al. Adaptive fractional-order switching-type control method design for 3D fractional-order nonlinear systems. Nonlinear Dyn. 2015;82(1):39-52.
33. Podlubny I. Fractional differential equations. Amsterdam: Elsevier; 1998.
34. Hangos KM, Bokor J, Szederkényi G. Analysis and control of nonlinear process systems. New York: Springer; 2006.
35. Slotine JJ, Li W. Applied nonlinear control. Englewood Cliffs, NJ: Prentice Hall; 1991.
36. Boudjedir CE, Boukhetala D, Bouri M. Nonlinear PD control of a parallel delta robot: experimental results. In: 2018 International Conference on Electrical Sciences and Technologies in Maghreb (CISTEM). IEEE; 2018: 1-4.
37. Wang J, Lee MC, Kim JH, Kim HH. Fast fractional-order terminal sliding mode control for seven-axis robot manipulator. Appl Sci. 2020;10:7757.
38. Li Y, Chen YQ, Podlubny I. Stability of fractional-order nonlinear dynamic systems: Lyapunov direct method and generalized Mittag-Leffler stability. Comput Math Appl. 2010;59:1810-21.
39. Boudjedir CE, Bouri M, Boukhetala D. Model-free iterative learning control with nonrepetitive trajectories for second-order MIMO nonlinear systems application to a delta robot. IEEE Trans Ind Electron. 2020;68(8):7433-43.
40. Jin M, Lee J, Chang PH, Choi C. Practical nonsingular terminal sliding-mode control of robot manipulators for high-accuracy tracking control. IEEE Trans Ind Electron. 2009;56(9):3593-601.

This work was supported by the DGRSDT of the Ministry of Higher Education and Scientific Research of Algeria.

Someya Amrane: https://orcid.org/0009-0008-0890-9047

Chems Eddine Boudjedir: https://orcid.org/0000-0002-4955-3728

Djamel Boukhetala: https://orcid.org/0000-0003-2112-0709